Received: 24 April 2023 | Revised: 6 November 2023 | Accepted: 9 November 2023

DOI: 10.1111/aec.13461

RESEARCH ARTICLE

From leaves to the whole tree: Mistletoe effects on the productivity, water relations, and demography of a Neotropical savanna tree

Mateus Cardoso Silva[1,2] | **Grazielle Sales Teodoro**[3] | **José Magno das Chagas Junior**[2] | **Sara Souza Bastos**[2] | **Joao Paulo Rodrigues Alves Delfino Barbosa**[4] | **Evaristo Mauro de Castro**[4] | **Marina Corrêa Scalon**[5] | **Eduardo van den Berg**[2]

[1]Department of Geography, College of Life and Environmental Sciences, University of Exeter, Exeter, UK

[2]Department of Ecology and Conservation, Federal University of Lavras, Lavras, Minas Gerais, Brazil

[3]Biological Sciences Institute, Federal University of Pará, Belém, Pará, Brazil

[4]Department of Biology, Federal University of Lavras, Lavras, Minas Gerais, Brazil

[5]Environmental Change Institute, School of Geography and the Environment, University of Oxford, Oxford, UK

Correspondence
Mateus Cardoso Silva, Department of Geography, College of Life and Environmental Sciences, University of Exeter, Laver Building, North Park Road, Exeter EX4 4QE, UK.
Email: mateuscardosobio@gmail.com

Funding information
Coordenação de Aperfeiçoamento de Pessoal de Nível Superior, Grant/Award Number: 001; Fundação de Amparo à Pesquisa do Estado de São Paulo, Grant/Award Number: 19/07773-1 and 19/24619-6; University of Exeter, Grant/Award Number: 710015629

Abstract

Trees' responses to mistletoes occur at multiple organization levels (e.g., leaf, individual, population), yet integrating these multi-scale responses is still challenging. Here, we compared the traits of infected versus uninfected trees over multiple scales, from leaf anatomy and physiology to canopy allometries and individual growth rate and survivorship. We tested the hypotheses that mistletoes lead in the host (1) the production of leaves with a conservative resource-use strategy, (2) more mechanically stable canopies and (3) reductions in growth and survival probability in the trees they infect. We addressed these hypotheses in the widespread savanna tree *Vochysia thyrsoidea* and xylem-tapping mistletoe *Psittacanthus robustus* in the Brazilian *Cerrado*, a global biodiversity hotspot. We found that (1) mistletoe infection did not affect key traits associated with resource conservativeness, such as leaf mass per area (LMA) and carbon assimilation rates (*A*). Likewise, (2) hosts did not increase the mechanical safety of their trunks in response to mistletoe infection since infected and uninfected trees had a similar allometric scaling between height and crown volume against stem diameter. (3) At the population level, both the relative growth rate and survival probability decreased as the number of parasites increased. However, zero growth and a 50% chance of mortality were estimated to occur in a minority of heavily infected trees (>7 and 14 parasites, respectively). Our results challenge the idea that mistletoes have a ubiquitous negative impact on their hosts. We highlight, therefore, the need for clarifying the mechanisms that allow trees to maintain their functioning even in the face of mistletoe parasitism.

KEYWORDS
Cerrado, hemiparasite, leaf economic spectrum, leaf gas exchange, Loranthaceae, mistletoe, population dynamics, tropical grassy ecosystems

INTRODUCTION

Natural enemies are key biotic drivers of plant function and mortality (Press & Phoenix, 2005). Parasitic plants, for instance, can affect tree physiology and demography, ultimately shaping vegetation dynamics, ecosystem

functioning and biogeochemical cycles (Watson, 2016). Mistletoes are photosynthesizing plant parasites (i.e., hemiparasites) belonging to the Loranthaceae and Santalaceae families. They grow specialized roots (i.e., haustorium) inside their hosts and uptake water and nutrients from the parasitized branches (Aukema, 2003). Consequently, these canopy-dwelling hemiparasites can create a water and nutritional deficit in the trees they infect (Cocoletzi et al., 2020; Griebel et al., 2022; Lüttge et al., 1998; Meinzer et al., 2004). Host responses to mistletoe infection are often examined at the leaf (Scalon & Wright, 2015; Silva et al., 2021; Wang et al., 2008) or branch level (Reblin & Logan, 2015; Sala et al., 2001; Tennakoon & Pate, 1996). Yet, it is still poorly known how mistletoe impacts reverberate across higher organizational levels, such as on host trees' architecture and demography. This knowledge gap limits our ability to assess host responses to mistletoes at the appropriate scales, further hampering our understanding of what drives or may disrupt the stable coexistence of mistletoes and their hosts.

At the leaf scale, due to the high resource demands by mistletoes, infected branches can produce leaves that optimize resource conservation instead of acquisition (Scalon et al., 2017). The conservative and acquisitive strategies characterize two ends of the leaf economic spectrum, a single axis representing the trade-off between leaf carbon costs and gains (Díaz et al., 2016; Oliveira et al., 2021; Reich, 2014). Leaf mass per area (LMA) is one of the key traits that distinguish conservative from acquisitive strategies at the leaf level. High LMA is often associated with low photosynthetic rates across taxonomic levels (Anderegg et al., 2018), characterizing the conservative end of the leaf economic spectrum (Wright et al., 2004). Changes in leaf anatomy may underlie LMA variation in response to mistletoe infection (Ozturk et al., 2019). High LMA can be achieved by reducing vessel size, which increases the density of xylem fibres and the safety of the leaf venation system against emboli formation and hydraulic failure (Blackman et al., 2010; Levionnois et al., 2021; Scoffoni et al., 2017). Increases in leaf thickness, especially the spongy mesophyll, can also lead to higher LMA (John et al., 2017; Poorter et al., 2009). Mistletoe-induced changes in leaf anatomy may allow leaves to operate under a more negative water potential (Scalon et al., 2017) to the detriment of maximum stomatal conductance and photosynthetic capacity, especially in nutrient-impoverished ecosystems (Oliveira et al., 2021).

Above the leaf level, mistletoes can modify the allometric relationship between the stem and canopy of their host trees. These parasites create not only water and nutrient deficits in their hosts but also add weight to the canopy of infected trees (Mylo et al., 2022). Mistletoes' extra weight can cause mechanical failure and branch breaching (Hadfield, 1999). Branch mortality can result in lower tree heights and smaller crowns relativized by stem diameter, leading to a more stable canopy (Aiba & Nakashizuka, 2009; Sellier & Fourcaud, 2009; van Gelder et al., 2006), despite the loss of the photosynthetic area in the canopy. It may be possible, therefore, that infected trees could respond to mistletoes' weight at the stem-crown allometries level, which may improve mechanical stability (Aiba & Nakashizuka, 2009; Sellier & Fourcaud, 2009; van Gelder et al., 2006).

At the individual scale, tree growth and survival probability are expected to decrease as the tree becomes heavily infected (Logan et al., 2013; Marias et al., 2014; Shaw et al., 2004, 2008; Teodoro et al., 2013). In fact, mistletoe outbreaks have contributed to major forest dieback in temperate forests (Bell et al., 2020; Griebel et al., 2017; Szmidla et al., 2019). Yet, understanding how mistletoes affect host population dynamics is still incipient in the tropics compared with temperate regions (Maponga et al., 2021; Monteiro et al., 2020).

Mistletoes can be found in a range of tropical ecosystems, being particularly common in savannas. 45% of mistletoe species recorded in Brazil (140 species) occur in the *Cerrado* (Reflora, 2020), a global biodiversity hotspot covered by fire- and edaphic-maintained savannas (Myers et al., 2000). Mistletoes have been reported to infect several of the dominant tree species in the *Cerrado* savannas, especially within the Vochysiaceae family (Arruda et al., 2012). For instance, there are registers of mistletoes from the *Psittacanthus* genus (Loranthaceae) parasitizing *Qualea grandiflora*, *Q. parviflora* and *Vochysia thyrsoidea* (Monteiro et al., 1992; Scalon & Wright, 2017; Teodoro et al., 2010), all widespread Vochysiaceae trees abundant where they occur (Bridgewater et al., 2004). Previous studies have shown that mistletoe can impair *V. thyrsoidea* carbon assimilation (Silva et al., 2021) and survivorship (Teodoro et al., 2013). However, to date, it is still missing an integrative approach linking tree responses to mistletoes across leaf, canopy and whole-tree scales in the *Cerrado* biodiversity hotspot.

Here, we investigated the effects of mistletoe on a widespread savanna tree in the Brazilian *Cerrado* to understand how and to what extent mistletoe infection could modulate host functioning from leaf to population metrics. Our model species were the tree *Vochysia thyrsoidea* Pohl (Vochysiaceae) and the mistletoe *Psittacanthus robustus* (Mart.) Marloth (Loranthaceae). We compiled unpublished data sets from three different sites containing traits from the leaf to the canopy and population scale between uninfected and infected individuals of *V. thyrsoidea* by *P. robustus*. We addressed the following hypotheses along with their respective predictions:

1. Mistletoe infection will shift the host leaf resource use towards the conservative end of the leaf economic spectrum. Infected individuals will have leaves with a low xylem vessel area (VA), palisade-to-spongy parenchyma ratio (P:S), carbon assimilation rate (*A*), and normalized difference vegetation index (NDVI) and higher mesophyll thickness (MT), leaf mass per area (LMA) and predawn/midday water potential (Ψ_{pd}/Ψ_{md}) compared with uninfected individuals.
2. The extra weight of mistletoes in the tree crown will lead to adjustments in the host stem-canopy allometries. Infected trees will have lower tree heights and crown volumes given a stem diameter at the breast height (DBH) compared with uninfected trees.
3. The intensity of mistletoe infection will negatively affect the host's growth and survivorship. Host relative growth rate inferred by DBH increment (RGR_{DBH}) and survival probability will decrease as the number of mistletoes increases.

MATERIALS AND METHODS

Study sites and sampling design

We studied three sites in the south of Minas Gerais state, Brazil, located in the transition between the *Cerrado* and Atlantic Rainforest (Figure 1a). The study sites were named *'Parque Ecológico Quedas do Rio Bonito'* (PEQRB), 'Carrancas Zilda' (CZ) and 'Carrancas Esmeralda' (CE). All study sites are fire-prone savannas (i.e., vegetation composed of a continuous grass layer with scattered trees) where rock outcrops also can be found. The PEQRB is located at 21°19′43.87″ S and 44°58′23.43″ W, 1024–1064 m altitude, Köppen climate classification Cwb-Cwa with 1529 mm annual cumulative rainfall, and 19°C annual mean temperature. CZ and CE are located at 21°28′16″ S and 44°37′21″ W and 21°27′59″ S and 44°42′10″

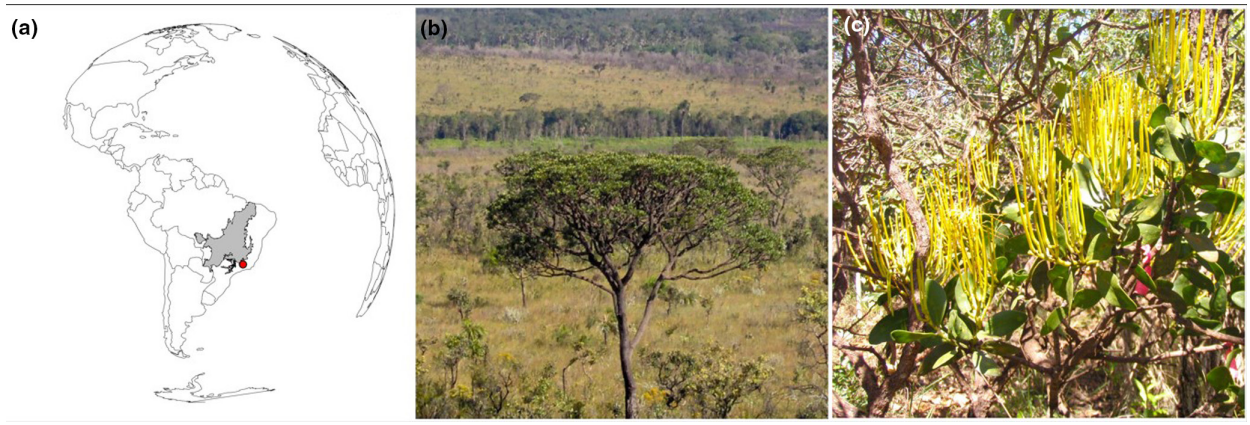

FIGURE 1 Study site and species. (a) The location of the studied savanna sites (red point) within the Brazilian *Cerrado* (grey). (b) *Vochysia thyrsoidea* tree in a typical savanna landscape. (c) *Psittacanthus robustus* mistletoe flowering.

W, at 1220 and 1044 m altitudes, respectively. Both sites' climates were classified as Cwa according to Köppen, with 1483 mm annual cumulative rainfall, and 14°C annual mean temperature. Three to four fires were registered in the PEQRB, two to three in CZ and two in CE from 1985 to 2020 according to MapBiomas Fire 1.0 (Alencar et al., 2020; Souza et al., 2020). Fire scars suggest that CZ burned in 2008 and CE in 2007 (personal observation). The minimum distance between the study sites was 0.08° and the maximum 0.36°.

We studied the foliar, allometric and demographic parameters of *V. thyrsoidea* (Figure 1b) uninfected or infected by *P. robustus* mistletoe (Figure 1c). Hereafter, 'uninfected' means *V. thyrsoidea* without any mistletoe attached to their branches and 'infected' were hosts with at least one mistletoe attached to their branches. Unfortunately, it was not possible to measure all traits at all sites in the same year due to financial and logistic constraints. However, the monthly mean temperature ($p = 0.23$) and precipitation ($p = 0.95$) did not vary while the data were being collected (Appendix S1), indicating that sampling at different years probably has a low impact on the conclusions we draw from data.

Leaf traits

Leaf anatomy and leaf mass per area

We measured leaf anatomical traits (mean vessel lumen area, VA; palisade-spongy parenchyma ratio, P:S; mesophyll thickness, MT) and leaf mass per area (LMA) in 10 infected and 10 uninfected trees at the PEQRB site in June 2016 (dry season). The LMA data are derived from Silva et al. (2021) while the VA, P:S and MT data are original. The number of mistletoes per infected tree ranged from 1 to 18, averaging 7.1 mistletoes per tree. The host selection criteria were stem diameter at breast height (1.3 m) (DBH) greater or equal to 4.7 cm, which corresponds to 15 cm of circumference. We selected only fully expanded sun leaves, between the 3rd and 5th node, and without traces of herbivory and pathogens. For infected individuals, leaves were taken from branches where there were mistletoes attached and preferentially in the twigs as close as possible to the parasite.

We sampled two leaves per tree for the anatomical measurements. We cut a rectangular sample (~2 cm wide × 4 cm long) in the median region of each leaf and fixed it in FAA 70% solution (formaldehyde, acetic acid and ethanol 70%, the ratio of 1:1:18). After 72 h, the samples were removed from

the FAA solution, washed and stored in ethanol 70%. For each sample, we made several transversal cuts in the midvein and leaf blade (cross-section) manually using a razor blade. All cuts were bleached using sodium hypochlorite and stained using a safrablau solution (1% safranin and 0.1% astrablau, the ratio of 7:1). We made glass slides for the best cuts (i.e., thin and semitransparent) and photographed them using a light microscope (Nikon Eclipse E100) connected to an image capture system (Nikon Infinity 1). We used the ImageJ software (1.52a) for all subsequent anatomical measurements.

We focussed on the abaxial part of the vascular cylinder (100× magnification) to measure vessel frequency (VF; i.e., number of vessels in the observational field) and total vessel area (TVA; i.e., the total area filled by vessel lumen in the observational field). We calculated the mean lumen area of an individual vessel (VA) by the following formula (Equation 1):

$$VA = \frac{TVA}{VF} \quad (1)$$

We focussed on the leaf blade (100× magnification) to measure the thickness of the mesophyll (MT), palisade parenchyma (PPT), and spongy parenchyma (SPT). We calculated the palisade-spongy parenchyma ratio (P:S) by the following formula (Equation 2):

$$P{:}S = \frac{PPT}{SPT} \quad (2)$$

We sampled five leaves per individual to measure LMA following the Pérez-Harguindeguy et al. (2013) protocol. Immediately after collecting the leaves in the field, we stored them in plastic bags in an ice-filled thermal box to avoid leaf dehydration and deformation during the transport from the field to the lab. In the laboratory, we let leaves rehydrate overnight by immersing them in water for at least 24 h at a low temperature (2 to 6°C). Then, we measured the water-saturated leaf area (LA) using a desk scanner (HP Scanjet 300) and we calculated the LA using the ImageJ software (1.52a). We let the leaves dry for 72 h at 70°C and then we measured their dry mass (LMdry) using a precision balance (Shimadzu AX200).

We calculated the LMA by the formula below (Equation 3).

$$LMA = \frac{LMdry}{LA} \quad (3)$$

Leaf carbon assimilation, reflectance, and water status

We measured the host leaf carbon assimilation rate (*A*), reflectance (normalized difference vegetation index, NDVI), and water potentials (predawn, Ψ_{pd}; midday Ψ_{md}) in 15 infected and 15 uninfected trees at the CZ site in August (dry season) and November (wet season) 2012. The number of mistletoes per infected tree was not available. The host selection criteria were tree height (*H*) greater than 2 m. Although the host selection criteria were tree height here and tree DBH for leaf anatomy and LMA, DBH and H were highly correlated (Pearson $r = 0.83$, $p < 0.001$, Appendix S2) and a DBH of 4.7 cm corresponds to *H* of 3.08 m (Appendix S2). Therefore, both criteria were deemed suitable to select individuals taller than 2 m. We sampled four green, healthy, sun, fully expanded (3rd–5th node) leaves per individual.

In the field, we collected the branch next to the mistletoe attachment and determined the leaf carbon assimilation rate (*A*) in the following 2 min. We utilized an LCA4 portable photosynthesis system (ADC Instruments) using ambient light and CO_2 supply ranging from 360 to 400 ppm. The measurements took place from 08:30 to 12:00 on sunny days only.

We collected another four leaves from the same branch and rapidly wrapped them in aluminium foil paper and stored them in an ice-filled thermal box. We quickly transported the leaves to the laboratory where it was possible to standardize the incident light source. We exposed the leaves to light radiation from 200 to 1005 nm and obtained their reflectance spectrum at a spectral resolution of 1 nm using a portable spectroradiometer (USB-850 RED TIDE) coupled to an electromagnetic radiation source (DT-MINI) and a reflectance probe (R400-7-VIS–NIR; US BioSolutions OceanOptics).

In addition to A, we used NDVI as a proxy of photosynthetic capacity (Barnes et al., 2017). We calculated the NDVI by the following formula (Equation 4; Gitelson & Merzlyak 1994):

$$\mathrm{NDVI} = \frac{(\mathrm{R750} - \mathrm{R705})}{(\mathrm{R750} + \mathrm{R705})} \tag{4}$$

where R750 and R705 are the leaf reflectance given to the 750 and 705 nm wavelength, respectively.

We measured the predawn (from 02:00 to 04:00) and midday water potential (from 11:00 to 13:00) in another four leaves in the same individuals using a pressure chamber (Model 1000 PMS Instruments).

Allometric relationships

We measured the allometric relationships between tree height (*H*), crown volume (CV) and stem diameter (DBH) in 60 infected and 60 uninfected trees (20 trees infected and 20 uninfected per study site) in all study sites (PEQRB, CZ, and CE) in 2012. The number of mistletoes per infected tree ranged from 1 to 6 averaging 1.65 mistletoes per tree. The host selection criteria were tree height greater than 2 m. For each tree, we measured tree height (*H*), stem diameter at breast height (1.30 m; DBH), the largest crown width (1CW), the crown width perpendicular to the greater one (2CW) and the crown depth (CD; i.e., the distance between the first branch ramification and the highest leaf in the crown). We estimated the crown volume (CV) by the following formula (Equation 5):

$$\mathrm{CV} = \frac{(\mathrm{1CW} \times \mathrm{2CW})}{2} \times \mathrm{CD} \tag{5}$$

Per-capita demographic parameters

We measured host growth rate and survival chance using a census of all *V. thyrsoidea* trees which fit the inclusion criteria ($H > 2$ m) over 8.4 hectares in all the study sites (PEQRB, CZ, and CE; 2.8 ha each) from 2007 to 2012. In the first survey, we tagged the trees, measured their initial DBH and recorded the initial number of mistletoes attached to the host crown. For further surveys, we re-measured the DBH and the number of mistletoes and registered the survival status (dead or alive) of each tree. The first survey in PEQRB was in March 2007 and we re-measured all live trees in September 2007, February 2008, September 2008, March 2009 and October 2009. The first survey in CZ was in September 2008 and we re-measured all live trees in January 2009, July 2009, January 2010, and February 2012. The first survey in CE was in August 2008 and we re-measured all live trees in March 2009, July 2010, November 2010 and January 2012. More information regarding the census from 2007 to 2010 can be found in Teodoro et al. (2010) and Teodoro et al. (2013), though the 2012 census is original to

this study. For each survey interval, we estimated the DBH-based relative growth rate by the following equation (Equation 6):

$$RGR_{DBH} = \frac{(DBH_i - DBH_{i-1})}{(t_i - t_{i-1})} \quad (6)$$

where DBH_i is the DBH of survey i, DBH_{i-1} is the DBH of the survey before i, t_i is the time of survey i and t_{i-1} is the time of the survey before i.

There were two types of pseudo-replication in the RGR_{DBH} data. First, there were from one to five values of RGR_{DBH} for the same tree as we measured RGR_{DBH} for each survey interval. Second, there was more than one RGR_{DBH} per survey interval for trees that had several branches at the breast height. We controlled the pseudo-replication issues by averaging RGR_{DBH} over time and among branches of the same tree. The survival chance was 0 for trees that died and 1 for trees that survived over the sampling period.

Data analysis

Hypothesis 1. We ran Student's *t*-tests and ANOVAs to test the hypothesis that mistletoes induce the production of conservative leaves in their hosts. We analysed VA, P:S, MT and LMA using Student's *t*-tests. The predictor variable was the mistletoe infection (uninfected vs. infected). We further investigated how gas exchange, reflectance and water potential traits responded to mistletoe infection over the seasons. For that, we analysed A, NDVI, Ψ_{pd}, and Ψ_{md} using two-way ANOVAs. The predictor variables were mistletoe infection, annual seasonality (dry season vs. wet season) and mistletoe infection × annual seasonality interaction. We first checked the normality and homoscedasticity assumptions of all traits through Shapiro–Wilk's and Lavene's tests, respectively (Appendix S3). When data did not fit the assumptions, we used the following logarithmic transformation, $f(x) = ln(x + 1)$, which linearized the response variable.

Hypothesis 2. We ran linear mixed-effect models to test the hypotheses that mistletoes reduce the slope between tree height and canopy size versus stem diameter. *H* and CV were the response variables, DBH the continuous predictor variable and infection status (infected vs. uninfected) the categorical predictor variable. The random effect was the study site. We can conclude that uninfected and infected trees have different H versus DBH or CV versus DBH slopes if the interaction term between DBH and infection status is statistically significant ($p < 0.05$). The relationship between CV versus DBH was nonlinear, so we applied a *ln* transformation to CV to meet the linearity assumption. For each model, we also estimated the marginal coefficient of determination (R^2_m, which includes only the fixed effects) and the conditional coefficient of determination (R^2_c, which includes both fixed and random effects). Taller *V. thyrsoidea* trees have been reported to be more likely to be infected by *P. robustus* (Teodoro et al., 2010). The size difference between infected versus uninfected trees could be a confusing factor when comparing their allometric relationships. A Student's *t*-test confirmed that infected trees had wider stems

than uninfected trees (Appendix S4). To control for that, we only included individuals with DBH < 30 cm to ensure both infected and uninfected trees have similar sizes.

Hypothesis 3. We fitted linear mixed-effect models to test the hypothesis that the infection degree impairs host growth and survival. The response variables were RGR_{DBH} and survival chance while the predictor variable was the number of mistletoes. We fitted a linear mixed-effect model (LMM) to RGR_{DBH} and a generalized linear mixed-effect model (GLMM; binomial family, logit link function) to survival chance. The random effect was the study site. We weighted the RGR_{DBH} observations by the number of censuses used to estimate the RGR_{DBH}. We also estimated the R^2_m and R^2_c of both models.

We performed all analyses in the R environment (version 4.1.0; Andy Bunn, 2017). We used the *lmer* and *glmer* functions from *lme4* package to fit the mixed-effect models (Bates et al., 2015). We used the *r.squaredGLMM* function from *MuMIn* package to estimate the R^2_m and R^2_c (Barton, 2022). We used the *leveneTest* function from the car package to run Levene's homoscedasticity test (Fox & Weisberg, 2019). We used the *cohens_d* function from the *effectsize* package (Ben-Shachar et al., 2020) and *pwr.t2n.test* function from the *pwr* package (Champely, 2020) to perform the power analysis.

RESULTS

Leaf structure, carbon relations and water status (Hypothesis 1)

There was no significant difference in the average vessel lumen area (VA; $t_{17.99} = 0.62$, $p = 0.53$), the ratio between palisade and spongy parenchyma (P:S; $t_{10.99} = 1.08$, $p = 0.3$) and the mesophyll thickness (MT; $t_{12.83} = 0.67$, $p = 0.51$) between uninfected and infected individuals (Figure 2a–c, Appendix S4). Similarly, the difference between the leaf mass per area (LMA) of uninfected (mean ± SD = 262.11 ± 43.49 g m^{-2}) and infected (301.51 ± 35.93, g m^{-2}) individuals was non-significant ($t_{13.66} = 2.02$, $p = 0.06$; Figure 2d, Appendix S5).

Mistletoe infection status (uninfected vs. infected), the season of the year (dry vs. wet) and their interaction did not affect the carbon assimilation rate (A; mistletoe: $F_{1,60} = 0.42$, $p = 0.51$; season: $F_{1,60} = 0.16$, $p = 0.68$; interaction: $F_{1,60} = 0.34$, $p = 0.55$) and normalized difference vegetation index (NDVI; mistletoe: $F_{1,60} = 0.28$, $p = 0.59$; season: $F_{1,60} = 0.02$, $p = 0.88$; interaction: $F_{1,60} = 0.04$, $p = 0.83$; Figure 2e, Appendix S6). The predawn leaf water potential (Ψ_{pd}) was higher (i.e., less negative; mistletoe: $F_{1,60} = 3.87$, $p = 0.05$) in infected individuals (mean ± SD = −0.29 ± 0.05 MPa) compared to uninfected individuals (−0.3 ± 0.05 MPa) and in the wet season (−0.26 ± 0.04 MPa) compared to the dry season (−0.32 ± 0.04 MPa; season: $F_{1,60} = 26.75$, $p < 0.001$; Figure 2f, Appendix S6). The interaction between infection status and season did not affect the Ψ_{pd} (interaction: $F_{1,60} = 0.38$, $p = 0.53$). The midday leaf water potential (Ψ_{md}) varied only between the dry versus wet season, but not between infected versus uninfected individuals (season: $F_{1,60} = 231.13$, $p < 0.001$; mistletoe: $F_{1,60} = 0.03$, $p = 0.84$; interaction: $F_{1,60} = 0.19$, $p = 0.65$; Figure 2g, Appendix S6). Specifically, the Ψ_{md} was higher during the wet season (−0.82 ± 0.23 MPa) than during the dry season (−2.1 ± 0.45 MPa).

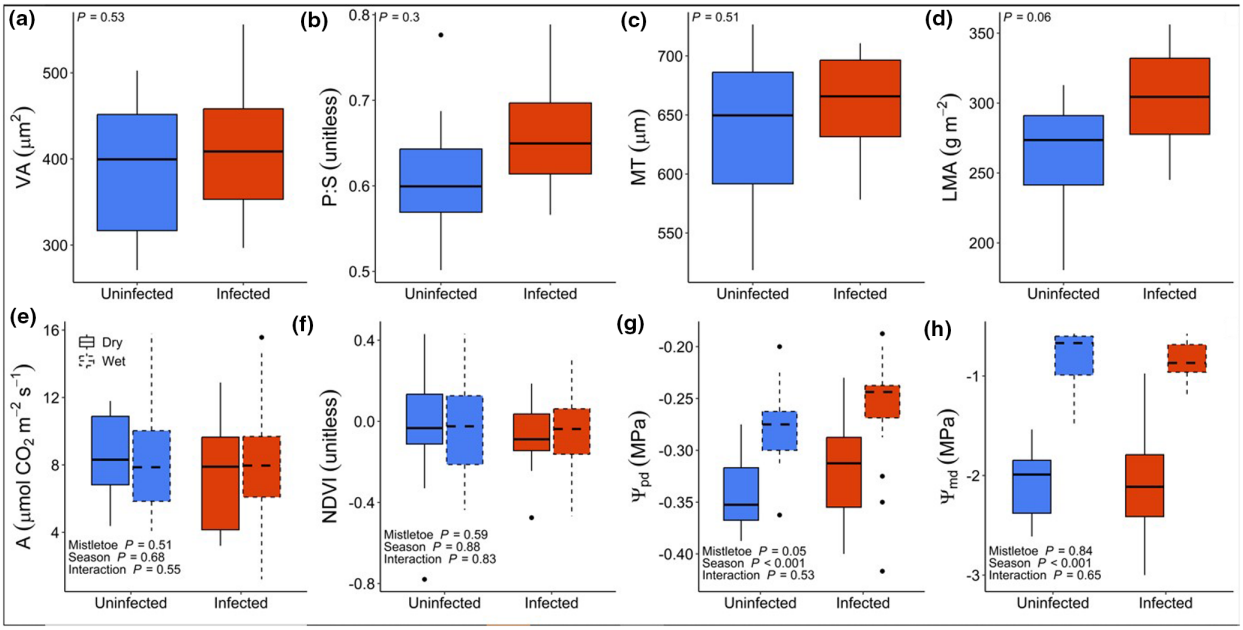

FIGURE 2 Leaf-level host responses to mistletoes. (a) Average xylem vessel area (VA), (b) ratio between palisade and spongy parenchyma (P:S), (c) mesophyll thickness (MT), and (d) leaf mass per area (LMA), (e) carbon assimilation rate (*A*), (f) normalized difference vegetation index (NDVI), (g) predawn water potential (Ψ_{pd}), and (h) midday water potential (Ψ_{md}) between uninfected (blue) and infected individuals (red) of *Vochysia thyrsoidea* by *Psittacanthus robustus*. The values of A, NDVI, Ψ_{pd}, and Ψ_{pd} during the dry and wet seasons were represented by a solid and dashed line, respectively. *p*-values on the top left corner of panels (a–d) refer to the *t*-tests between uninfected versus infected individuals. *p*-values of panels (e–g) refer to the ANOVAs where infection status ('Mistletoe', uninfected vs. infected), the season of the year ('Season', dry vs. wet), and their interaction ('Interaction') were the predictor variables.

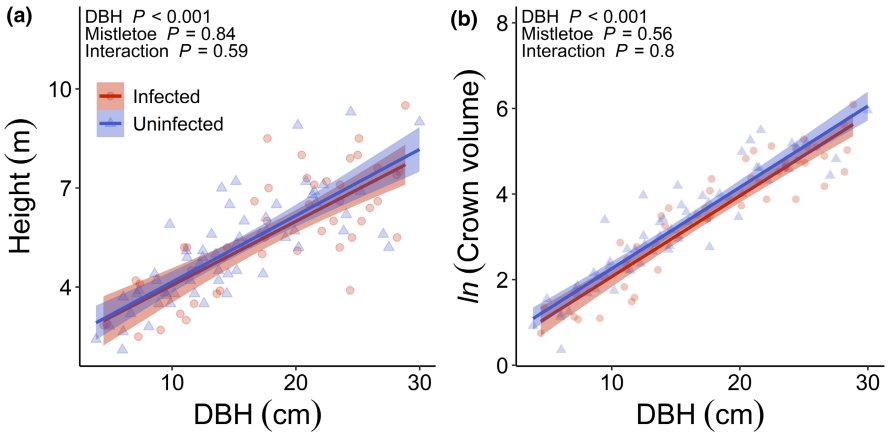

FIGURE 3 Mistletoe effects on host stem and canopy allometries. (a) The relationship between tree height and the stem diameter at the breast height (DBH). (b) The relationship between crown volume natural algorithm and DBH. The *p*-values associated with the predictor variables on the top left corner. Red circles represent infected and blue triangles uninfected individuals. 'Mistletoe' represents the infection status (uninfected vs. infected) and 'Interaction' the DBH × Mistletoe interaction. Only individuals with DBH < 30 cm were included in the analysis.

Stem and canopy allometric scaling (Hypothesis 2)

Mistletoe infection did not affect the allometric scaling of tree height and crown volume versus stem diameter (Figure 3, Appendix S7). Tree height and crown volume natural logarithm increased linearly with DBH (tree height: estimate = 0.18 ± 0.02 SE, $t_{105.81} = 9.11$, $p < 0.001$; *ln* crown volume: 0.18 ± 0.01, $t_{106.69} = 18.54$, $p < 0.001$). The infection status (infected vs. uninfected) did not have a statistically significant effect on tree height (−0.09 ± 0.51, $t_{104.33} = -0.19$, $p = 0.84$) and *ln* crown volume (0.14 ± 0.25,

$t_{104.62} = 0.58$, $p = 0.56$). Similarly, the interaction term between DBH and infection status did not significantly affect the tree height versus DBH (0.01 ± 0.02, $t_{104.2} = 0.53$, $p = 0.59$) and *ln* crown volume versus DBH relationships (0.003 ± 0.01, $t_{104.4} = 0.24$, $p = 0.8$). The fixed effects (R^2_m) explained 61% and 86% of the tree height versus DBH and *ln* crown volume versus DBH models, respectively. The percentage of variance explained increased to 66% and 87% considering fixed plus random effects (R^2_c) in the same comparison.

Tree growth and survivorship (Hypothesis 3)

The number of mistletoes decreased both the host relative growth rate (RGR_{DBH}; slope estimate ± SE = -0.03 ± 0.01, $t_{605.97} = -2.43$, $p = 0.01$) and survival chance (-0.31 ± 0.06, $z = -4.57$, $p < 0.001$; Figure 4, Appendix S8). None of the sampled trees died at the 'CE' site during the study. Therefore, we ran a second model excluding for "CE" site and the results were qualitatively similar to the full model (-0.29 ± 0.06, $z = 4.3$, $p < 0.001$; Appendix S8). The mean number of mistletoes per tree was 0.69. Approximately 67% of all sampled trees remained uninfected throughout the study (416 of 614 trees). Only 1% were parasitized by up to five mistletoes during the study, with the mean number of mistletoes in infected individuals being 2.15. RGR_{DBH} tended to be negative after *c*. 7 mistletoes infected the host canopy (Figure 4a). Survival chance tended to be 98% in uninfected individuals and below 50% in individuals infected by up to *c*. 14 mistletoes (Figure 4b). The number of mistletoes alone (R^2_m) explained, respectively, 0.3% and 5% of host RGR_{DBH} and survival chance. Whereas the number of mistletoes along with the study site as the random effect (R^2_c) explained, respectively, 2% and 42% of host RGR_{DBH} and survival chance.

DISCUSSION

Here, we compile data at multiple scales of plant functioning to assess the effects of mistletoe on a tropical tree from leaf anatomical structure to population dynamics. Contrary to previous expectations, we found that (1) mistletoes did not induce conservative resource use in the leaves of the branches

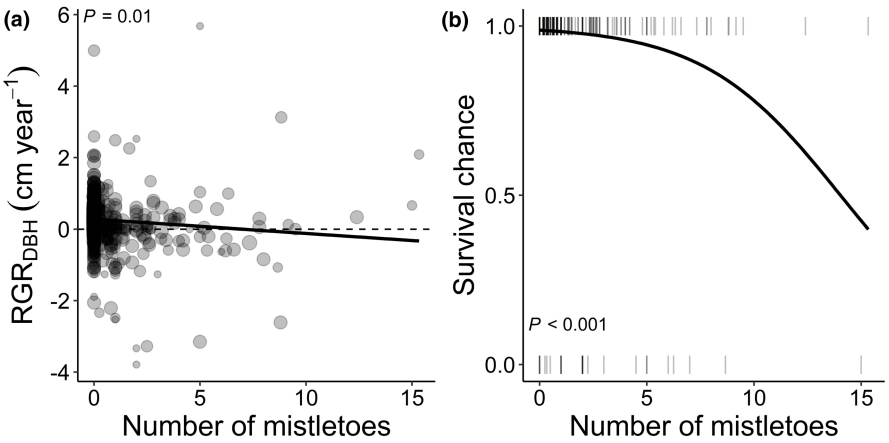

FIGURE 4 Mistletoe effects on host demography. (a) Relative growth rate based on the stem diameter at breast height variation (RGR_{DBH}) and (b) survival status (alive: 1, dead: 0) as a function of the average number of mistletoes from 2007 to 2012. The point size in (a) is proportional to the number of time intervals used for calculating the RGR_{DBH} (ranging from 1 to 5 intervals) and the dashed line marks the zero. The vertical bars in (b) represent the observations. Line equation in (a) $0.27606 - 0.03946 \times x$; logistic curve equation in (b) $\frac{e^{4.40158 - 0.31374 \times x}}{1 + e^{4.40158 - 0.31374 \times x}}$, where *x* is the number of mistletoes.

they are attached to. Leaf mass per area was not sensitive to infection status. (2) Mistletoe infection did not affect tree architecture. Tree height- and crown volume-stem diameter allometries were similar between infected and uninfected individuals. Furthermore, although (3) mistletoes negatively affected tree growth and survivorship, the number of parasites was far from being the main driver of the host demography. Below, we discuss the mismatch between prior expectations and our findings, moving towards a more mechanistic understanding of how mistletoes and trees interact.

Leaf-level responses to mistletoes

Contrary to Hypothesis 1, the presence of mistletoe did not induce host trees to produce more sclerophyllous leaves (low VA and P:S and high MT) with low photosynthetic capacities (e.g., low A and NDVI) and high LMA. An increase in the host LMA due to mistletoe parasitism was observed in other Neotropical savanna trees, such as *Eremanthus erythropappus* infected by *Phoradendron crassifolium* (Silva et al., 2021) and *Handroanthus chrysotrichus* infected by *Phoradendron affine* (Scalon et al., 2017). The distinctive pattern found here can emerge from three non-exclusive causes. First, *V. thyrsoidea* leaves may have a limited acclimation potential. *V. thyrsoidea* has one of the highest LMA among dominant Neotropical savanna species, including the ones cited above (Batalha et al., 2011). Therefore, increasing LMA even further can be constrained by the fact that *V. thyrsoidea* already produces extremely sclerophyllous leaves. Second, the studied mistletoe, *P. robustus*, may not cause sufficient stress (in low loads) to induce changes in their hosts at the leaf level. *P. robustus* belongs to the Loranthaceae family, a less aggressive mistletoe family compared to Viscaceae (Scalon & Wright, 2015), the family where the *Phoradendron* genus belongs. Third, the populational oscillation of *P. robustus* may reduce the chance of this parasite inducing leaf structural modifications in their hosts. *V. thyrsoidea* produces longevous leaves, with an average leaf lifespan of 2 years (Rossatto, 2013). Meanwhile, the populations of *P. robustus* fluctuate over time, especially due to fire events leading to widespread mortality of those parasites (Teodoro et al., 2013). It might be more likely to observe mistletoe-induced changes in host leaf structure in species with more acquisitive leaves, infected by mistletoes that are more efficient in draining host resources (e.g., *Phoradendron* spp. and others Viscaceae) and persisting in the host branch for a longer time.

The lack of a significant effect of mistletoe parasitism on host photosynthesis contradicts previous studies in the same species pair. Silva et al. (2021) found that *V. thyrsoidea* trees infected by *P. robustus* had a carbon assimilation rate (*A*) approximately half lower (average of 7.2 μmol CO^2 $m^{-2}s^{-1}$) than uninfected trees (average of 11.6 μmol CO^2 $m^{-2}s^{-1}$). In the present study, infected and uninfected *V. thyrsoidea* trees had a statistically similar A, averaging at 8.2 μmol CO^2 $m^{-2}s^{-1}$. Soil nutrients and moisture are known to vary drastically over a few metres in *Cerrado* landscapes (Abrahão et al., 2019; Lira-Martins et al., 2022; Mattos et al., 2023). Since the studies were carried out in different sites, it might be possible that fine-scale edaphic gradients influence the effects of mistletoes on their host productivity. In addition to site-specific differences, we speculate that different infection intensities might underlie the sensitivity of tree photosynthetic rates to mistletoes (Queijeiro-Bolaños et al., 2020; Sala et al., 2001). Unfortunately, data on the number and volume of mistletoes per host were not available either here or in Silva et al. (2021). Future studies could unveil the causes of this inconsistency by testing whether edaphic conditions and parasite loads shape tree photosynthetic responses to mistletoes.

Predawn leaf water potential (Ψ_{pd}) was marginally less negative in infected individuals compared to uninfected ones irrespective of the season, contradicting previous studies (Ehleringer et al., 1986; Griebel et al., 2022; Scalon et al., 2021). This suggests that *V. thyrsoidea* leaves under mistletoe influence have virtually similar water status to leaves from trees without mistletoe over the entire year. Two non-exclusive hypotheses may explain this finding. First, *P. robustus* colonization success may be higher in branches with a better water status within the host canopy. The water potential of the host branches is known to affect mistletoe colonization and physiology (Bickford et al., 2005; Scalon et al., 2016). If that applies to our model species, the slightly higher water potentials under the mistletoe influence may reflect the parasite infection success rather than a host response. Alternatively, the most impaired branches by the mistletoe may not be the ones that the parasite is attached to, but in fact, 'healthy' branches neighbouring the infected ones (Silva et al., 2021). These hemiparasites may redirect the water to the infected branches due to their extra leaf area and high transpiration rates, indirectly benefiting the leaves in infected branches (Silva et al., 2021). In this scenario, the water status of leaves under mistletoe infection might be paradoxically improved compared to uninfected trees, as it was found here and in a temperate conifer previously (Logan et al., 2013). Further research can test the proposed hypotheses by modelling mistletoe infection success as a function of host branch physiological status and monitoring sap flow rates between healthy and infected branches within infected trees.

Impacts of mistletoes on tree canopies

We found no evidence that trees adjust their stem allometries to compensate for mistletoe mechanical stress, refuting Hypothesis 2. Although we do not have data on mistletoe size, previous studies show that *P. robustus* crowns can grow up to 2.3 m wide (Teodoro et al., 2010), which certainly creates tension in the infected branch. Yet, the *P. robustus* crown width is directly proportional to the *V. thyrsoidea* branch diameter (Teodoro et al., 2010). Thus, mistletoes probably grow big in large branches only, which may be wider enough to neutralize mistletoe mechanical stress. Furthermore, mistletoes induce branch hypertrophy (Mylo et al., 2021) and increased lignification (Hu et al., 2017), which also reduces the risk of infected branches breaking (Muche et al., 2022). Finally, most of the studied infected individuals had between one and two mistletoes attached to their crowns, a range that was consistent with the average infection degree from our census (2.15 mistletoes per tree). We can, therefore, only conclude that tree architecture is insensitive to mistletoe infection under low parasite densities. Whether this holds up under high parasite density/volumes is an outstanding hypothesis to be tested. In summary, not only mistletoes did not affect most of the analysed host leaf traits, but also no effects were detected looking at the height-crown-stem allometric scaling.

Tree demography under mistletoe parasitism

Supporting Hypothesis 3, the number of mistletoes slightly decreased the host growth rate and the likelihood of survival (Bell et al., 2020; Logan et al., 2013; Shaw et al., 2008). However, *P. robustus* effects on *V. thyrsoidea* growth and mortality occurred only at high parasite densities. More than seven parasites were needed to lead to negative tree growth rates and up to 14 mistletoes were required to reduce survival probability below 50%.

Yet, only 1% out of the 614 studied trees had more than five mistletoes parasitizing their canopies. Hence, most of the *V. thyrsoidea* trees studied here were below the threshold required for mistletoes significantly affecting their demography, suggesting that *P. robustus* is not a threat to the studied *V. thyrsoidea* populations. Moreover, differences between sites captured by R^2_c explained 6- to 8-fold more the host growth and survival variability than mistletoe infection degree alone (R^2_m). Thereby, differences across regions due to fire regimes and soil types, for instance, are more likely to drive the productivity and mortality of *V. thyrsoidea* than mistletoe infection exclusively. Mistletoe outbreaks have been responsible for major forest dieback in temperate regions (Szmidla et al., 2019; Tamudo et al., 2021), especially among conifers (Dobbertin & Rigling, 2006; Scott & Mathiasen, 2012). But in tropical savannas, it might be possible that the coexistence between mistletoes and their hosts is more stable probably due to the long-term coevolution (Jerome & Ford, 2002; Medel et al., 2010) and fire events controlling mistletoe populations (Teodoro et al., 2013).

Concluding remarks and future perspectives

Our findings challenge the conception that mistletoes have pervasive impacts on parasitized branches leaves and tree architecture (see Koenig et al., 2018). Leaf traits either remained unchanged (VA, P:S, MT, LMA, A, NDVI, and Ψ_{md}) or had slightly improved values (high Ψ_{pd}) in response to the mistletoe parasitism. Host trees did not adjust the allometric scaling between canopy height and volume versus stem diameter to counterbalance the mechanical stress induced by the parasites. Infected trees grew less and were more likely to die, but only for a minority of trees extremely infected by mistletoes. Future studies should consider multiple scales to investigate the effects of mistletoe on their host trees, as was done here. Our approach allowed us to detect mistletoe impacts on tree growth and mortality under heavy parasite loads (individual scale), without major changes in leaf anatomy and physiology (leaf scale) and stem allometries (canopy scale). These findings point to a stable coexistence between host trees and mistletoes. As long as mistletoe loads remain low (e.g., less than seven *P. robustus* per *V. thyrsoidea*), mistletoe's contributions to ecosystem multifunctionality—through resource provisioning to bird species, for instance—do not imply host tree population declines. Outstanding questions are as follows: Does the position of the host tree within the leaf economic spectrum shape its foliar responses to mistletoes? Do parasitized branches respond to mistletoe infection by changes in wood structural and chemical properties? Does fire maintain a stable coexistence between mistletoes and their host species across fire-prone ecosystems?

AUTHOR CONTRIBUTIONS

Mateus Cardoso Silva: Conceptualization (lead); data curation (lead); formal analysis (lead); investigation (equal); methodology (lead); project administration (supporting); writing – original draft (lead); writing – review and editing (lead). **Grazielle Sales Teodoro:** Conceptualization (equal); data curation (equal); funding acquisition (equal); investigation (equal); methodology (equal); project administration (equal); writing – original draft (equal); writing – review and editing (equal). **José Magno das Chagas Junior:** Data curation (equal); investigation (equal); methodology (equal). **Sara Souza Bastos:** Data curation (equal); investigation (equal); methodology (equal). **João Paulo Rodrigues Alves Delfino Barbosa:** Funding acquisition (equal); resources (equal); writing – original draft (equal); writing – review and editing (equal). **Evaristo Mauro de**

Castro: Funding acquisition (equal); resources (equal). **Marina Corrêa Scalon:** Writing – original draft (equal); writing – review and editing (equal). **Eduardo van den Berg:** Conceptualization (equal); funding acquisition (lead); methodology (equal); project administration (equal); resources (equal); supervision (lead); writing – original draft (equal); writing – review and editing (equal).

ACKNOWLEDGEMENTS

We thank Ítalo A. Fernandes for the assistance in the anatomical analyses. We are grateful for field support by the members of the van den Berg's laboratory, especially Flávia F. Siqueira and Renato Q. Furtado. We acknowledge Joana N. Brockmeyer and Marcelo Rodrigues for their assistance with the gas exchange and reflectance analyses. We are grateful to anonymous reviewers who helped to improve the quality of the manuscript.

FUNDING INFORMATION

This study was funded by the Fundação de Amparo à Pesquisa do Estado de São Paulo (19/24619–6), Coordenação de Aperfeiçoamento de Pessoal de Nível Superior, Brasil (001) and University of Exeter studentship (710015629).

CONFLICT OF INTEREST STATEMENT

The authors declare that they have no conflict of interest.

DATA AVAILABILITY STATEMENT

The data used in the manuscript is available on https://figshare.com/projects/Neotrop_Mistletoe/187140.

ORCID

Mateus Cardoso Silva https://orcid.org/0000-0002-5528-8828
Joao Paulo Rodrigues Alves Delfino Barbosa https://orcid.org/0000-0002-2624-966X
Marina Corrêa Scalon https://orcid.org/0000-0003-2069-8226
Eduardo van den Berg https://orcid.org/0000-0002-0843-6437

REFERENCES

Abrahão, A., Costa, P.B., Lambers, H., Andrade, S.A.L., Sawaya, A.C.H.F., Ryan, M.H. et al. (2019) Soil types select for plants with matching nutrient-acquisition and -use traits in hyperdiverse and severely nutrient-impoverished Campos rupestres and cerrado in Central Brazil. *Journal of Ecology*, 107(3), 1302–1316. Available from: https://doi.org/10.1111/1365-2745.13111

Aiba, M. & Nakashizuka, T. (2009) Architectural differences associated with adult stature and wood density in 30 temperate tree species. *Functional Ecology*, 23(2), 265–273. Available from: https://doi.org/10.1111/j.1365-2435.2008.01500.x

Alencar, A.A., Conciani, D.E., Costa, D.P., Rosa, E.R., Martin, E.V., Hasenack, H. et al. (2020) *MapBiomas fire collection 1.0 version 1*. Available at: https://mapbiomas-br-site.s3.amazonaws.com/Metodologia/FOGO/ATBD_-_MapBiomas_Fogo_-_Coleção_1.pdf [Accessed: 23rd March 2023].

Anderegg, L.D.L., Berner, L.T., Badgley, G., Sethi, M.L., Law, B.E. & HilleRisLambers, J. (2018) Within-species patterns challenge our understanding of the leaf economics spectrum. *Ecology Letters*, 21(5), 734–744. Available from: https://doi.org/10.1111/ele.12945

Andy Bunn, M.K. (2017) *A language and environment for statistical computing*. Vienna: R Foundation for Statistical Computing, pp. 11–18. Available at: http://www.r-project.org [Accessed: 20th September 2018].

Arruda, R., Fadini, R.F., Carvalho, L.N., del-Claro, K., Mourão, F.A., Jacobi, C.M. et al. (2012) Ecology of neotropical mistletoes: an important canopy-dwelling component of Brazilian ecosystems. *Acta Botanica Brasilica*, 26(2), 264–274. Available from: https://doi.org/10.1590/S0102-33062012000200003

Aukema, J.E. (2003) Vectors, Viscin, and Viscaceae: mistletoes as parasites, mutualists, and resources. *Frontiers in Ecology and the Environment*, 1(4), 212. Available from: https://doi.org/10.2307/3868066

Barnes, M.L., Breshears, D.D., Law, D.J., van Leeuwen, W.J.D., Monson, R.K., Fojtik, A.C. et al. (2017) Beyond greenness: detecting temporal changes in photosynthetic capacity with hyperspectral reflectance data. *PLoS One*. Edited by K. P. Vadrevu, 12(12), e0189539. Available from: https://doi.org/10.1371/journal.pone.0189539

Barton, K. (2022) *MuMIn: Multi-Model Inference*. Available at: https://cran.r-project.org/package=MuMIn [Accessed: 26th April 2022].

Batalha, M.A., Silva, I.A., Cianciaruso, M.V. & de Carvalho, G.H. (2011) Trait diversity on the phylogeny of cerrado woody species. *Oikos*, 120(11), 1741–1751. Available from: https://doi.org/10.1111/j.1600-0706.2011.19513.x

Bates, D., Mächler, M., Bolker, B. & Walker, S. (2015) Fitting linear mixed-effects models using lme4. *Journal of Statistical Software*, 67(1), 1–48. Available from: https://doi.org/10.18637/jss.v067.i01

Bell, D.M., Pabst, R.J. & Shaw, D.C. (2020) Tree growth declines and mortality were associated with a parasitic plant during warm and dry climatic conditions in a temperate coniferous forest ecosystem. *Global Change Biology*, 26(3), 1714–1724. Available from: https://doi.org/10.1111/gcb.14834

Ben-Shachar, M.S., Lüdecke, D. & Makowski, D. (2020) Effectsize: estimation of effect size indices and standardized parameters. *Journal of Open Source Software*, 5(56), 2815. Available from: https://doi.org/10.21105/joss.02815

Bickford, C.P., Kolb, T.E. & Geils, B.W. (2005) Host physiological condition regulates parasitic plant performance: *Arceuthobium vaginatum* subsp. cryptopodum on *Pinus ponderosa*. *Oecologia*, 146(2), 179–189. Available from: https://doi.org/10.1007/s00442-005-0215-0

Blackman, C.J., Brodribb, T.J. & Jordan, G.J. (2010) Leaf hydraulic vulnerability is related to conduit dimensions and drought resistance across a diverse range of woody angiosperms. *New Phytologist*, 188(4), 1113–1123. Available from: https://doi.org/10.1111/j.1469-8137.2010.03439.x

Bridgewater, S., Ratter, J.A. & Ribeiro, J.F. (2004) Biogeographic patterns, –diversity and dominance in the cerrado biome of Brazil. *Biodiversity and Conservation*, 13(12), 2295–2317. Available from: https://doi.org/10.1023/B:BIOC.0000047903.37608.4c

Champely, S. (2020) *pwr: Basic Functions for Power Analysis*. Available at: https://cran.r-project.org/package=pwr [Accessed: 23rd March 2023].

Cocoletzi, E., Angeles, G., Briones, O., Ceccantini, G. & Ornelas, J.F. (2020) The ecophysiology of a neotropical mistletoe depends on the leaf phenology of its tree hosts. *American Journal of Botany*, 107(9), 1225–1237. Available from: https://doi.org/10.1002/ajb2.1529

Díaz, S., Kattge, J., Cornelissen, J.H.C., Wright, I.J., Lavorel, S., Dray, S. et al. (2016) The global spectrum of plant form and function. *Nature*, 529(7585), 167–171. Available from: https://doi.org/10.1038/nature16489

Dobbertin, M. & Rigling, A. (2006) Pine mistletoe (*Viscum album* ssp. *austriacum*) contributes to scots pine (*Pinus sylvestris*) mortality in the Rhone valley of Switzerland. *Forest Pathology*, 36(5), 309–322. Available from: https://doi.org/10.1111/j.1439-0329.2006.00457.x

Ehleringer, J.R., Cook, C.S. & Tieszen, L.L. (1986) Comparative water use and nitrogen relationships in a mistletoe and its host. *Oecologia*, 68(2), 279–284. Available from: https://doi.org/10.1007/BF00384800

Fox, J. & Weisberg, S. (2019) *An R companion to applied regression*. Third. Thousand Oaks, CA: Sage. Available at: https://socialsciences.mcmaster.ca/jfox/Books/Companion/

Gitelson, A. & Merzlyak, M.N., (1994). Spectral reflectance changes associated with autumn senescence of *Aesculus hippocastanum* L. and *Acer platanoides* L. leaves. Spectral features and relation to chlorophyll estimation. *Journal of Plant Physiology*, 143(3), 286–292. https://doi.org/10.1016/S0176-1617(11)81633-0

Griebel, A., Peters, J.M.R., Metzen, D., Maier, C., Barton, C.V.M., Speckman, H.N. et al. (2022) Tapping into the physiological responses to mistletoe infection during heat and drought stress. *Tree physiology*, 42(3), 523–536. Available from: https://doi.org/10.1093/treephys/tpab113

Griebel, A., Watson, D. & Pendall, E. (2017) Mistletoe, friend and foe: synthesizing ecosystem implications of mistletoe infection. *Environmental Research Letters*, 12(11), 115012. Available from: https://doi.org/10.1088/1748-9326/aa8fff

Hadfield, J.S. (1999) Douglas-fir dwarf mistletoe infection contributes to branch breakage. *Western Journal of Applied Forestry*, 14(1), 5–6. Available from: https://doi.org/10.1093/wjaf/14.1.5

Hu, B., Sakakibara, H., Takebayashi, Y., Peters, F.S., Schumacher, J., Eiblmeier, M. et al. (2017) Mistletoe infestation mediates alteration of the phytohormone profile and antioxidative metabolism in bark and wood of its host *Pinus sylvestris*. *Tree Physiology*, 37(5), 676–691. Available from: https://doi.org/10.1093/treephys/tpx006

Jerome, C.A. & Ford, B.A. (2002) The discovery of three genetic races of the dwarf mistletoe *Arceuthobium americanum* (Viscaceae) provides insight into the evolution of parasitic angiosperms. *Molecular Ecology*, 11(3), 387–405. Available from: https://doi.org/10.1046/j.0962-1083.2002.01463.x

John, G.P., Scoffoni, C., Buckley, T.N., Villar, R., Poorter, H. & Sack, L. (2017) The anatomical and compositional basis of leaf mass per area. *Ecology letters*, 20(4), 412–425. Available from: https://doi.org/10.1111/ele.12739

Koenig, W.D., Knops, J.M.H., Carmen, W.J., Pesendorfer, M.B. & Dickinson, J.L. (2018) Effects of mistletoe (*Phoradendron villosum*) on California oaks. *Biology Letters*, 14(6), 20180240. Available from: https://doi.org/10.1098/rsbl.2018.0240

Levionnois, S., Jansen, S., Wandji, R.T., Beauchêne, J., Ziegler, C., Coste, S. et al. (2021) Linking drought-induced xylem embolism resistance to wood anatomical traits in Neotropical trees. *New Phytologist*, 229(3), 1453–1466. Available from: https://doi.org/10.1111/nph.16942

Lira-Martins, D., Nascimento, D.L., Abrahão, A., de Britto Costa, P., D'Angioli, A.M., Valézio, E. et al. (2022) Soil properties and geomorphic processes influence vegetation composition, structure, and function in the Cerrado Domain. *Plant and Soil*, 476(1–2), 549–588. Available from: https://doi.org/10.1007/s11104-022-05517-y

Logan, B.A., Reblin, J.S., Zonana, D.M., Dunlavey, R.F., Hricko, C.R., Hall, A.W. et al. (2013) Impact of eastern dwarf mistletoe (*Arceuthobium pusillum*) on host white spruce (*Picea glauca*) development, growth and performance across multiple scales. *Physiologia Plantarum*, 147(4), 502–513. Available from: https://doi.org/10.1111/j.1399-3054.2012.01681.x

Lüttge, U., Haridasan, M., Fernandes, G.W., de Mattos, E.A., Trimborn, P., Franco, A.C. et al. (1998) Photosynthesis of mistletoes in relation to their hosts at various sites in tropical Brazil. *Trees*, 12(3), 167. Available from: https://doi.org/10.1007/s004680050136

Maponga, T.S., Ndagurwa, H.G.T. & Witkowski, E.T.F. (2021) Functional and species composition of understory plants varies with mistletoe-infection on *Vachellia karroo* trees in a semi-arid African savanna. *Global Ecology and Conservation*, 32, e01897. Available from: https://doi.org/10.1016/j.gecco.2021.e01897

Marias, D.E., Meinzer, F.C., Woodruff, D.R., Shaw, D.C., Voelker, S.L., Brooks, J.R. et al. (2014) Impacts of dwarf mistletoe on the physiology of host *Tsuga heterophylla* trees as recorded in tree-ring C and O stable isotopes. *Tree Physiology*, 34(6), 595–607. Available from: https://doi.org/10.1093/treephys/tpu046

Mattos, C.R.C., Mazzochini, G.G., Rius, B.F., Penha, D., Giacomin, L.L., Flores, B.M. et al. (2023) Rainfall and topographic position determine tree embolism resistance in Amazônia and Cerrado sites. *Environmental Research Letters*, 18(11), 114009. Available from: https://doi.org/10.1088/1748-9326/ad0064

Medel, R., Mendez, M.A., Ossa, C.G. & Botto-Mahan, C. (2010) Arms race coevolution: the local and geographical structure of a host–parasite interaction. *Evolution: Education and Outreach*, 3(1), 26–31. Available from: https://doi.org/10.1007/s12052-009-0191-7

Meinzer, F.C., Woodruff, D.R. & Shaw, D.C. (2004) Integrated responses of hydraulic architecture, water and carbon relations of western hemlock to dwarf mistletoe infection. *Plant, Cell and Environment*, 27(7), 937–946. Available from: https://doi.org/10.1111/j.1365-3040.2004.01199.x

Monteiro, G.F., Novais, S., Barbosa, M., Antonini, Y., Passos, M.F.O. & Wilson Fernandes, G. (2020) The mistletoe *Struthanthus flexicaulis* reduces dominance and increases diversity of plants in campo rupestre. *Flora*, 271(June), 151690. Available from: https://doi.org/10.1016/j.flora.2020.151690

Monteiro, R.F., Martins, R.P. & Yamamoto, K. (1992) Host specificity and seed dispersal of *Psittacanthus robustus* (Loranthaceae) in south-East Brazil. *Journal of Tropical Ecology*, 8(3), 307–314. Available from: https://doi.org/10.1017/S026646740000657X

Muche, M., Muasya, A.M. & Tsegay, B.A. (2022) Biology and resource acquisition of mistletoes, and the defense responses of host plants. *Ecological Processes*, 11(1), 24. Available from: https://doi.org/10.1186/s13717-021-00355-9

Myers, N., Mittermeier, R.A., Mittermeier, C.G., da Fonseca, G.A.B. & Kent, J. (2000) Biodiversity hotspots for conservation priorities. *Nature*, 403(6772), 853–858. Available from: https://doi.org/10.1038/35002501

Mylo, M.D., Hofmann, M., Balle, F., Beisel, S., Speck, T. & Speck, O. (2022) Biomechanics of the parasite–host interaction of the European mistletoe. *Journal of Experimental botany*, 73(4), 1204–1221. Available from: https://doi.org/10.1093/jxb/erab518

Mylo, M.D., Hofmann, M., Delp, A., Scholz, R., Walther, F., Speck, T. et al. (2021) Advances on the visualization of the internal structures of the European mistletoe: 3D reconstruction using microtomography. *Frontiers in Plant Science*, 12, 1–13. Available from: https://doi.org/10.3389/fpls.2021.715711

Oliveira, R.S., Eller, C.B., Barros, F.V., Hirota, M., Brum, M. & Bittencourt, P. (2021) Linking plant hydraulics and the fast–slow continuum to understand resilience to drought in tropical ecosystems. *New Phytologist*, 230(3), 904–923. Available from: https://doi.org/10.1111/nph.17266

Ozturk, M., Coskuner, K.A., Usta, Y., Serdar, B. & Bilgili, E. (2019) The effect of mistletoe (*Viscum album*) on branch wood and needle anatomy of scots pine (*Pinus sylvestris*). *IAWA Journal*, 40(2), 352–365. Available from: https://doi.org/10.1163/22941932-40190219

Pérez-Harguindeguy, N., Díaz, S., Garnier, E., Lavorel, S., Poorter, H., Jaureguiberry, P. et al. (2013) New handbook for standardised measurement of plant functional traits worldwide. *Australian Journal of Botany*, 61(3), 167. Available from: https://doi.org/10.1071/BT12225

Poorter, H., Niinemets, Ü., Poorter, L., Wright, I.J. & Villar, R. (2009) Causes and consequences of variation in leaf mass per area (LMA): a meta-analysis. *New Phytologist*, 182(3), 565–588. Available from: https://doi.org/10.1111/j.1469-8137.2009.02830.x

Press, M.C. & Phoenix, G.K. (2005) Impacts of parasitic plants on natural communities. *New Phytologist*, 166(3), 737–751. Available from: https://doi.org/10.1111/j.1469-8137.2005.01358.x

Queijeiro-Bolaños, M.E., Malda-Barrera, G.X., Carrillo-Angeles, I.G. & Suzán-Azpiri, H. (2020) Contrasting gas exchange effects on the interactions of two mistletoe species and their host *Acacia schaffneri*. *Journal of Arid Environments*, 173, 104041. Available from: https://doi.org/10.1016/j.jaridenv.2019.104041

Reblin, J.S. & Logan, B.A. (2015) Impacts of eastern dwarf mistletoe on the stem hydraulics of red spruce and white spruce, two host species with different drought tolerances and responses to infection. *Trees*, 29(2), 475–486. Available from: https://doi.org/10.1007/s00468-014-1125-8

Reflora. (2020) *Brazilian Flora 2020*. Available at: http://floradobrasil.jbrj.gov.br/reflora/PrincipalUC/PrincipalUC.do [Accessed 6th October 2021].

Reich, P.B. (2014) The world-wide "fast-slow" plant economics spectrum: a traits manifesto. *Journal of Ecology*, 102(2), 275–301. Available from: https://doi.org/10.1111/1365-2745.12211

Rossatto, D.R. (2013) Seasonal patterns of leaf production in co-occurring trees with contrasting leaf phenology: time and quantitative divergences. *Plant Species Biology*, 28(2), 138–145. Available from: https://doi.org/10.1111/j.1442-1984.2012.00373.x

Sala, A., Carey, E.V. & Callaway, R.M. (2001) Dwarf mistletoe affects whole-tree water relations of Douglas fir and western larch primarily through changes in leaf to sapwood ratios. *Oecologia*, 126(1), 42–52. Available from: https://doi.org/10.1007/s004420000503

Scalon, M.C., dos Reis, S.A. & Rossatto, D.R. (2017) Shifting from acquisitive to conservative: the effects of *Phoradendron affine* (Santalaceae) infection in leaf morpho-physiological traits of a Neotropical tree species. *Australian Journal of Botany*, 65(1), 31. Available from: https://doi.org/10.1071/BT16177

Scalon, M.C., Rossatto, D.R., Domingos, F.M.C.B. & Franco, A.C. (2016) Leaf morpho-physiology of a Neotropical mistletoe is shaped by seasonal patterns of host leaf phenology. *Oecologia*, 180(4), 1103–1112. Available from: https://doi.org/10.1007/s00442-015-3519-8

Scalon, M.C., Rossatto, D.R. & Franco, A.C. (2021) How does mistletoe infection affect seasonal physiological responses of hosts with different leaf phenology? *Flora*, 281, 151871. Available from: https://doi.org/10.1016/j.flora.2021.151871

Scalon, M.C. & Wright, I.J. (2015) A global analysis of water and nitrogen relationships between mistletoes and their hosts: broad-scale tests of old and enduring hypotheses. *Functional Ecology*, 29(9), 1114–1124. Available from: https://doi.org/10.1111/1365-2435.12418

Scalon, M.C. & Wright, I.J. (2017) Leaf trait adaptations of xylem-tapping mistletoes and their hosts in sites of contrasting aridity. *Plant and Soil*, 415(1–2), 117–130. Available from: https://doi.org/10.1007/s11104-016-3151-3

Scoffoni, C., Albuquerque, C., Brodersen, C.R., Townes, S.V., John, G.P., Cochard, H. et al. (2017) Leaf vein xylem conduit diameter influences susceptibility to embolism and hydraulic decline. *New Phytologist*, 213(3), 1076–1092. Available from: https://doi.org/10.1111/nph.14256

Scott, J.M. & Mathiasen, R.L. (2012) Assessing growth and mortality of bristlecone pine infected by dwarf mistletoe using dendrochronology. *Forest Science*, 58(4), 366–376. Available from: https://doi.org/10.5849/forsci.10-142

Sellier, D. & Fourcaud, T. (2009) Crown structure and wood properties: influence on tree sway and response to high winds. *American Journal of Botany*, 96(5), 885–896. Available from: https://doi.org/10.3732/ajb.0800226

Shaw, D.C., Huso, M. & Bruner, H. (2008) Basal area growth impacts of dwarf mistletoe on western hemlock in an old-growth forest. *Canadian Journal of Forest Research*, 38(3), 576–583. Available from: https://doi.org/10.1139/X07-174

Shaw, D.C., Watson, D.M. & Mathiasen, R.L. (2004) Comparison of dwarf mistletoes (*Arceuthobium* spp., Viscaceae) in the western United States with mistletoes (*Amyema* spp., Loranthaceae) in Australia—ecological analogs and reciprocal models for ecosystem management. *Australian Journal of Botany*, 52(4), 481. Available from: https://doi.org/10.1071/BT03074

Silva, M.C., Guimarães, A.F., Teodoro, G.S., Bastos, S.S., de Castro, E.M. & van den Berg, E. (2021) The enemy within: the effects of mistletoe parasitism on infected and uninfected host branches. *Plant Ecology*, 222(5), 639–645. Available from: https://doi.org/10.1007/s11258-021-01132-6

Souza, C.M., Shimbo, J.Z., Rosa, M.R., Parente, L.L., Alencar, A.A., Rudorff, B.F. et al. (2020) Reconstructing three decades of land use and land cover changes in Brazilian biomes with Landsat archive and earth engine. *Remote Sensing*, 12(17), 2735. Available from: https://doi.org/10.3390/rs12172735

Szmidla, H., Tkaczyk, M., Plewa, R., Tarwacki, G. & Sierota, Z. (2019) Impact of common mistletoe (*Viscum album* L.) on scots pine forests—a call for action. *Forests*, 10(10), 847. Available from: https://doi.org/10.3390/f10100847

Tamudo, E., Camarero, J.J., Sangüesa-Barreda, G. & Anadón, J.D. (2021) Dwarf mistletoe and drought contribute to growth decline, dieback and mortality of junipers. *Forests*, 12(9), 1199. Available from: https://doi.org/10.3390/f12091199

Tennakoon, K.U. & Pate, J.S. (1996) Effects of parasitism by a mistletoe on the structure and functioning of branches of its host. *Plant, Cell and Environment*, 19(5), 517–528. Available from: https://doi.org/10.1111/j.1365-3040.1996.tb00385.x

Teodoro, G.S., van den Berg, E. & Arruda, R. (2013) Metapopulation dynamics of the mistletoe and its host in Savanna areas with different fire occurrence. *PLoS One*, 8(6), e65836. Available from: https://doi.org/10.1371/journal.pone.0065836

Teodoro, G.S., van den Berg, E., de Castro Nunes Santos, M. & de Freitas Coelho, F. (2010) How does a *Psittacanthus robustus* Mart. Population structure relate to a *Vochysia thyrsoidea* Pohl. Host population? *Flora - Morphology, Distribution, Functional Ecology of Plants*, 205(12), 797–801. Available from: https://doi.org/10.1016/j.flora.2010.04.013

van Gelder, H.A., Poorter, L. & Sterck, F.J. (2006) Wood mechanics, allometry, and life-history variation in a tropical rain forest tree community. *New Phytologist*, 171(2), 367–378. Available from: https://doi.org/10.1111/j.1469-8137.2006.01757.x

Wang, L., Kgope, B., D'Odorico, P. & Macko, S.A. (2008) Carbon and nitrogen parasitism by a xylem-tapping mistletoe (*Tapinanthus oleifolius*) along the Kalahari transect: a stable isotope study. *African Journal of Ecology*, 46(4), 540–546. Available from: https://doi.org/10.1111/j.1365-2028.2007.00895.x

Watson, D.M. (2016) Fleshing out facilitation – reframing interaction networks beyond top-down versus bottom-up. *New Phytologist*, 211(3), 803–808. Available from: https://doi.org/10.1111/nph.14052

Wright, I.J., Reich, P.B., Westoby, M., Ackerly, D.D., Baruch, Z., Bongers, F. et al. (2004) The worldwide leaf economics spectrum. *Nature*, 428(6985), 821–827. Available from: https://doi.org/10.1038/nature02403

How to cite this article:
Silva, M.C., Teodoro, G.S., Junior, J.M.d.C., Bastos, S.S., Barbosa, J.P.R.A.D., de Castro, E.M. et al. (2023) From leaves to the whole tree: Mistletoe effects on the productivity, water relations, and demography of a Neotropical savanna tree. *Austral Ecology*, 00, 1–18. Available from: https://doi.org/10.1111/aec.13461

SUPPORTING INFORMATION

Additional supporting information can be found online in the Supporting Information section at the end of this article.